The Mast Cell Function-Associated Antigen and Its Interactions with the Type I Fcε Receptor †

ARTICLE *in* MOLECULAR IMMUNOLOGY · OCTOBER 2002

Impact Factor: 2.97 · DOI: 10.1021/bi011566i · Source: PubMed

6 AUTHORS, INCLUDING:

Guy M Hagen
University of Colorado Colorado Springs
48 PUBLICATIONS **267** CITATIONS

PERGAMON

Molecular Immunology 38 (2001) 1315–1321

Molecular Immunology

www.elsevier.com/locate/molimm

Interactions of the mast cell function-associated antigen with the type I Fcε receptor

Jinming Song [a], Guy Hagen [b], Steven M.L. Smith [a], Deborah A. Roess [a], Israel Pecht [c], B. George Barisas [b,*]

[a] *Department of Physiology, Colorado State University, Fort Collins, CO 80523, USA*
[b] *Department of Chemistry, Colorado State University, Fort Collins, CO 80523, USA*
[c] *Department of Immunology, Weizmann Institute of Science, 76100 Rehovot, Israel*

Received 31 December 2001; accepted 18 January 2002

Abstract

Clustering the mast cell function-associated antigen (MAFA), a membrane glycoprotein expressed on 2H3 cells, by its specific monoclonal antibody G63 substantially inhibits secretion normally triggered by aggregating these cells' Type I Fcε receptor (FcεRI). To explore possible MAFA-FcεRI interactions giving rise to this inhibition, we have studied by time-resolved phosphorescence anisotropy the rotational behavior of both MAFA and FcεRI as ligated by various reagents involved in FcεRI-induced degranulation and MAFA-mediated inhibition thereof. From 4 to 37 °C the rotational correlation times (mean ± S.D.) of FcεRI-bound, erythrosin-conjugated IgE resemble those observed for MAFA-bound erythrosin-conjugated G63 Fab, 82±17 μs and 79±31 μs at 4 °C, respectively. Clustering the FcεRI-IgE complex by antigen or by anti-IgE increases the phosphorescence anisotropy of G63 Fab and slows its rotational relaxation. Lateral diffusion of G63 Fab is also slowed by antigen clustering of the receptor. Taken together, these results suggest that unperturbed MAFA associates with clustered FcεRI. They are also consistent with its interaction with the isolated receptor, a situation also suggested by FRET measurements on the system.

Keywords: 2H3; Degranulation; Raft; Rotation; Photobleaching

1. Introduction

The mast cell function-associated antigen or MAFA is a membrane glycoprotein of 2H3 mast cells capable of modulating these cells' FcεRI-mediated secretory response (Ortega and Pecht, 1988). Pecht and coworkers identified MAFA as the target of the mAb G63 which inhibits RBL-2H3 cell degranulation induced by FcεRI clustering. Although at most one MAFA is expressed for every 10 FcεRI, clustering MAFA using the specific mAb G63 inhibits by up to 80% the secretory response of 2H3 cells to subsequent FcεRI clustering (Ortega and Pecht, 1988). The question of how such a protein, expressed in sub-stoichiometric amounts, can deliver negative signals overriding those of the aggregated FcεRI is difficult to answer. MAFA aggregation inhibits both the FcεRI-induced signaling cascade upstream of PLCγ activation, namely suppressing both phosphatidylinositide phosphate hydrolysis and transient intracellular calcium elevation (Guthmann et al., 1995b; Ortega and Pecht, 1988). The inhibitory effect of mAb G63 requires MAFA clustering and is not due to interference with IgE-FcεRI interactions (Ortega and Pecht, 1988).

MAFA is a 28–40 kDa glycoprotein when expressed as a monomer and also exists as a disulfide-linked homodimer (Ortega and Pecht, 1988). It is a 188 amino acids long, type II integral membrane glycoprotein (Guthmann et al., 1995a) whose C-terminal (extracellular) domain exhibits homology to calcium-dependent animal lectins including the type II FcεRI (CD23) and the natural killer cell receptors. MAFA's 34 amino acid cytoplasmic tail contains a SIYSTL sequence, an immunoreceptor tyrosine-based inhibitory motif (ITIM), the tyrosine of which is at least partly phosphorylated upon its clustering (Guthmann et al., 1995a; Rong and Pecht,

Abbreviations: 2H3 cell, rat mucosal mast cell of the RBL-2H3 line; BCR, B cell receptor; Er, erythrosin isothiocyanate; CTB, cholera toxin B subunit; FcεRI, type I (high affinity) Fcε receptor; FPR, fluorescence photobleaching recovery; FRET, fluorescence resonant energy transfer; ITAM, immunoreceptor tyrosine-based activation motif; ITIM, immunoreceptor tyrosine-based inhibitory motif; mAb, monoclonal antibody; MAFA, mast cell function-associated antigen; PBS, phosphate-buffered saline; TPA, time-resolved phosphorescence anisotropy

* Corresponding author. Tel.: +1-970-491-6641; fax: +1-970-491-1801.
E-mail address: barisas@lamar.colostate.edu (B.G. Barisas).

0161-5890/02/$ – see front matter © 2002 Elsevier Science Ltd. All rights reserved.
PII: S0161-5890(02)00081-0

1996). The tyrosine-phosphorylated ITIM serves, in turn, to bind and activate both SHP-2 (Xu and Pecht, 2001) and SHIP (Xu et al., 2001). The latter phosphatase appears to be the primary enzyme responsible for MAFA's inhibitory action.

Previous studies suggest certain parameters of interactions between FcεRI and MAFA, the membrane localization of these species, and the linkage of these interactions to the aggregation state of the molecular species: (1) unperturbed, non-aggregated FcεRI are dispersed within the plasma membrane (Kubitscheck et al., 1991) but, upon aggregation, are translocated into lipid rafts as has been shown by Baird's group (Field et al., 1995); (2) the Jovin laboratory has demonstrated fluorescence resonant energy transfer (FRET) between FcεRI-bound IgE and MAFA-bound intact G63 mAb and shown that this energy transfer is not increased upon FcεRI clustering (Jurgens et al., 1996). Unfortunately, in this study, receptor interactions with unclustered MAFA, as probed by G63Fab, were not examined; and (3) 2H3 cell degranulation is apparently triggered by bifunctional antibodies specific for FcεRI and MAFA (Schweitzer-Stenner et al., 1999) which implies the existence of pre-existing MAFA-FcεRI aggregates.

We may hypothesize, reasoning from the above FRET and bifunctional antibody results, that MAFA is at least partly associated with the FcεRI, irrespective of the latter's aggregation state. Such a circumstance could be tested by measuring the in-membrane motions of MAFA and the receptor. If MAFA is constitutively associated with the FcεRI, then TPA and FPR measurements on the MAFA-FcεRI system should yield certain specific results, given that the receptor is present in large excess: (1) MAFA should exhibit the same apparent rotational correlation time as the FcεRI and this value should be too large for an isolated molecule of MAFA's size; (2) aggregating the receptor into large clusters should reduce the lateral diffusion coefficients of both MAFA and the receptor; (3) such treatment should rotationally immobilize both MAFA and the receptor, thus increasing the limiting anisotropies of both species; and (4) FRET should be observed from MAFA-bound G63 Fab to FcεRI-bound IgE.

2. Materials and methods

2.1. Antibodies and proteins

mAb G63 (IgG_1) used in the present studies was purified from hybridoma culture supernatants by chromatography on protein A-Sepharose and Fab and F(ab′)2 fragments prepared by proteolytic digestion (Song et al., 2002). Monoclonal DNP-specific A2 rat IgE was purified from ascitic fluid by binding to DNP-Sepharose and elution with DNP-glycine (Soto and Pecht, 1988). 95.3 anti-mouse IgE was purified as previously described (Baniyash and Eshhar, 1984). Goat anti-mouse IgG (Fab-specific; M6898), rabbit anti-mouse IgG (M7023), goat anti-mouse IgG (Fc-specific; M2650) and goat anti-DNP IgG (D9781) antibodies were obtained from Sigma, St. Louis, MO. DNP_{11}-BSA, derivatized with an average of 11 DNP-groups per molecule, was prepared as described earlier (Carsten and Eisen, 1953).

Antibodies were derivatized with erythrosin isothiocyanate (Er; Molecular Probes, Eugene, OR) using a modification (Song et al., 2002) of methods described by Johnson and Holborow (Johnson and Holborow, 1986). Monofunctional Cy3 and Alexa 488 were purchased from Amersham Pharmacia Biotech (Piscataway, NJ) and Molecular Probes (Eugene, OR), respectively, and used according to Manufacturers' directions. Prior to use, all dye-derivatized proteins were centrifuged at $130,000 \times g$ for 10 min in a Beckman Airfuge (Beckman Instruments, Palo Alto, CA) to remove any protein aggregates formed during storage.

2.2. RBL-2H3 cells

Rat mucosal-type mast cells of the RBL-2H3 line were kindly provided by Dr. Reuben Siraganian of the National Institutes of Health and grown and characterized as described (Song et al., 2002). Cells were labeled with fluorescent or phosphorescent protein conjugates using 150 nM IgE or 30 nM G63 mAb, Fab or $(Fab')_2$ at 4 °C for 1 h. Prior to phosphorescence measurements, cells were deoxygenated to eliminate phosphorescence quenching by O_2 (Johnson and Garland, 1981).

2.3. Biophysical measurements

Time-resolved phosphorescence anisotropy (TPA) experiments were performed using methods previously described (Barisas et al., 1999; Philpott et al., 1995) as adapted for MAFA (Song et al., 2002). Phosphorescence from deoxygenated cell samples was excited by 532 nm pulses from a Nd:YAG laser. Phosphorescence emitted polarized parallel $I_{\parallel}(t)$ and perpendicular $I_{\perp}(t)$ to the exciting light were analyzed to yield a phosphorescence intensity function $s(t) = I_{\parallel}(t) + 2I_{\perp}(t)$ and a phosphorescence anisotropy function $r(t) = [I_{\parallel}(t) - I_{\perp}(t)]/s(t)$. Anisotropy data were analyzed according to a single average exponential decay model $r(t) = r_{\infty} + (r_0 - r_{\infty})\exp(-t/\varphi)$ which yielded the initial anisotropy value r_0, the limiting anisotropy value r_{∞} and the rotational correlation time φ (Song et al., 2002). Fluorescence photobleaching recovery measurements (FPR) of membrane protein lateral diffusion were performed using the interference fringe method (Munnelly et al., 1998) which provides extraordinarily high sensitivity for measurements on sparsely-expressed membrane proteins like MAFA. From the measured time at which fluorescence recovery is half-complete and from the known optical parameters, the diffusion constant and the fraction of labeled molecules mobile on the experimental timescale were then evaluated. Efficiency of fluorescence resonant energy transfer was measured using donor photobleaching methods described previously (Young et al., 1994) and analyzed by a global

procedure simultaneously comparing normalized donor and donor plus acceptor photobleaching traces through non-linear least squares analysis to obtain a single %*E*.

2.4. Density gradient centrifugation

Cell samples ((25–50) × 10^6) saturated with A2-IgE (100 mM, 30 min 25 °C) were treated with DNP-BSA (200 ng/ml, 30 min, 37 °C) to cluster FcεRI or with intact G63 mAb (100 nM, 30 min, 37°) to aggregate MAFA. After washing, cells were lysed with 0.25% Triton X-100 and subjected to sucrose density gradient centrifugation as described by Baird's group (Field et al., 1995). The resulting gradient was divided into 12 fractions, 40 μl aliquots of which were electrophoresed on non-reducing gradient gels, transferred to nitrocellulose and probed with 1:1000 dilutions of G63 anti-MAFA, J17 anti-FcεRI or 95-3 anti-IgE followed by 1:10,000 dilution of horseradish peroxidase-conjugated anti-mouse IgG. Blots were incubated 5 min with "Super Signal West Pico" chemiluminescence detection substrate and recorded by 1–5 min exposure on Amersham Enhanced ECL film.

3. Results

3.1. FcεRI-bound IgE and MAFA-bound G-63 Fab behave similarly as unconstrained membrane proteins in time-resolved phosphorescence anisotropy experiments

Fig. 1 presents a comparison of TPA measurement results for FcεRI-bound IgE and MAFA-bound G63 Fab at 4 °C. The rotational correlation times for FcεRI-bound IgE and for MAFA-bound G-63 Fab are virtually identical at 82 ± 17 μs (mean ± S.D. not S.E.M.) and 79 ± 31 μs, respectively. Rotational correlation times also decrease with increasing temperature (Fig. 1 inset). For IgE this decrease is from 82 μs at 4 °C to 27 μs at 37 °C, i.e. about three-fold over this temperature range. In contrast, the initial and limiting anisotropies change very little over this range. MAFA's rotational correlation time changes similarly, from 79 μs at 4 °C to 38 μs at 37 °C.

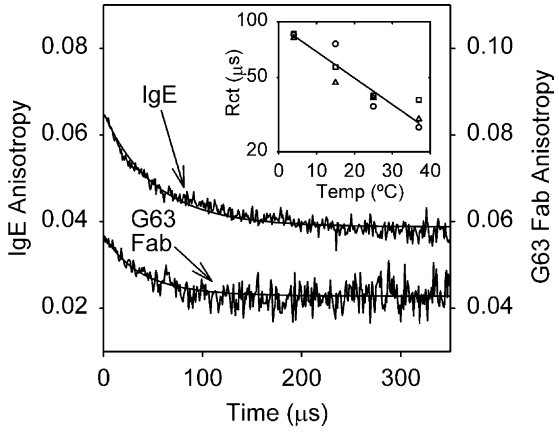

Fig. 1. Anisotropy decay kinetics for Er-IgE and Er-G63 Fab bound to 2H3 cells at 4 °C. Traces shown are averages of 21 experiments (IgE) and 23 experiments (G63). The inset shows the temperature dependence of rotational correlation times for the above species as well as Er-G63 intact mAb. Symbols in inset graph: (○), IgE; (□), G63Fab; (△), G63 mAb. All points are satisfactorily fitted by a single curve with rotational correlation times of 84 μs at 4 °C and 28 μs at 37 °C. This corresponds to an activation energy of 5.9 kcal mol^{-1}, a value typical of diffusive flow in membranes.

A value of 60 μs for the FcεRI rotational correlation time at 4 °C has been predicted based on the receptor's size and structure (Song et al., 2002) and the observed value of 82 μs agrees well quite with this figure. The rotational correlation time to be expected for MAFA depends upon whether the monomer or the disulfide-linked dimer is the prevalent form. MAFA dimer rotation might be expected to resemble that of class II molecules, being similar in size and possessing two transmembrane segments. Rotational correlation times averaging 10–20 μs at 4 °C have been measured for a number of wild-type and cytoplasmically-truncated I-A^k and I-A^d species (Barisas et al., 1999; Munnelly et al., 2000). Hence the rotational correlation times of FcεRI and MAFA dimers would be expected to differ substantially (60–80 vis à vis 10–20 μs) with a correspondingly larger difference expected for monomeric MAFA molecules. By contrast, the rotational correlation times of unperturbed FcεRI-bound IgE and MAFA-bound G63 Fab are indistinguishable (82 and 79 μs, respectively). Intrinsic association of MAFA with FcεRI is thus consistent with these results.

3.2. MAFA rotation and lateral diffusion are restricted by FcεRI clustering

A fundamental question is whether MAFA, when not aggregated, is nonetheless associated with FcεRI. We therefore measured the rotational motions of MAFA binding G63 Fab before and after FcεRI aggregation by antigen or anti-IgE. Averages of several anisotropy decay traces for MAFA rotation on cells variously treated and probed with Er-conjugated G63 Fab are shown in Fig. 2. These traces show that FcεRI clustering by DNP_{11}-BSA produces a substantial increase in the anisotropy of G63 Fab from 0.045 to 0.053 while aggregation of MAFA via G63 Fab and polyclonal anti-IgG produces a somewhat larger increase.

An effect of FcεRI aggregation on MAFA lateral diffusion was also observed. Clustering FcεRI by DNP_{11}-BSA reduced MAFA's diffusion coefficient from $(2.2 \pm 0.5) \times 10^{-10}$ on untreated cells to $(0.8 \pm 0.5) \times 10^{-10}$ cm^2 s^{-1} after treatment. Fig. 3 shows the visible slowing of MAFA fluorescence recovery after photobleaching on FcεRI-clustered cells. As would be expected, aggregating MAFA through G63Fab and anti-IgG produced a much larger effect on the MAFA diffusion coefficient, reducing it almost 10-fold to $(0.18 \pm 0.04) \times 10^{-10}$ cm^2 s^{-1}.

These rotation measurements clearly suggest either that aggregating FcεRI-induces interactions between the receptor

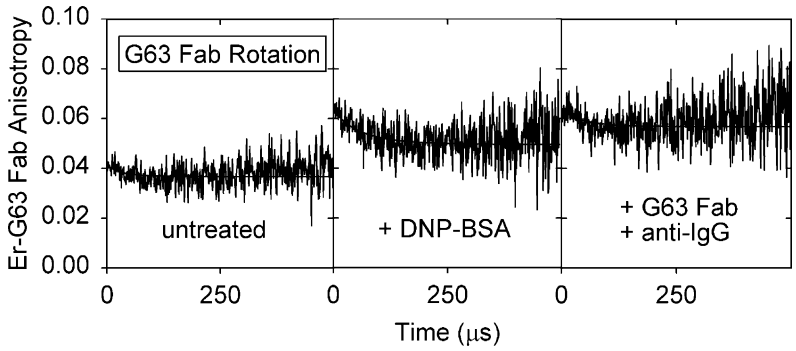

Fig. 2. Effects of FcεRI and MAFA crosslinking on MAFA rotational diffusion at 4 °C as probed by Er-G63 Fab. Traces shown are averages of three to six independent measurements. FcεRI crosslinking by DNP_{11}-BSA and direct crosslinking of MAFA by G63 Fab and polyclonal anti-IgG increase MAFA rotational correlation time from 79 to 110 μs and 151 μs, respectively. FcεRI crosslinking by DNP_{11}-BSA produces a small but consistent increase in MAFA limiting anisotropy from 0.045 to 0.053 while direct MAFA crosslinking produces a larger increase in this quantity to 0.063. Both of these effects demonstrate restriction of MAFA rotation by either treatment.

and G63 Fab-binding MAFA or that these interactions already exist with unclustered FcεRI. In either case, the restriction of MAFA rotation caused by FcεRI clustering would directly reflect the lower mobility of aggregated FcεRI. By contrast, the rotational diffusion parameters of MAFA when binding intact mAb G63 are virtually identical in the presence and absence of FcεRI clustering. Further support for the interaction of MAFA with (at least) aggregated FcεRI comes from the lateral diffusion measurements of MAFA. Fig. 3 shows a substantial slowing of MAFA's lateral diffusion upon antigen treatment, though the effect is not nearly as pronounced at that induced by direct aggregation of MAFA using G63 Fab and anti-IgG. Such behavior would be observed if a substantial fraction of MAFA molecules were intrinsically associated with both isolated and aggregated FcεRI.

3.3. MAFA-bound G63 Fab Exhibits FRET to IgE

Efficiency of FRET from Alexa 488-conjugated G63 Fab to Cy3-conjugated IgE was measured using donor photobleaching methods. Rates of donor photobleaching are reduced in the presence of FRET to acceptor chromophores and such behavior is clearly shown in Fig. 4. MAFA-bound G63 Fab exhibits 17 ± 8% spontaneous FRET to FcεRI-bound IgE. Small, but not statistically significant, increases in FRET were observed after DNP-BSA treatment or if G63 mAb was employed (data not shown). These results point to constitutive association of at least a fraction of MAFA with FcεRI and so suggest that FRET observed by Jovin and colleagues (Jurgens et al., 1996) between FcεRI-bound IgE and MAFA-bound intact G63 mAb does not fundamentally require MAFA crosslinking by bivalent antibody or other means.

3.4. The Fcγ domain of mAb G63 apparently interacts with additional 2H3 cell surface receptors

G63 inhibition of 2H3 cell degranulation was originally discovered as an effect of cell treatment with the intact mAb (Soto and Pecht, 1988). Although clustering G63 Fab was

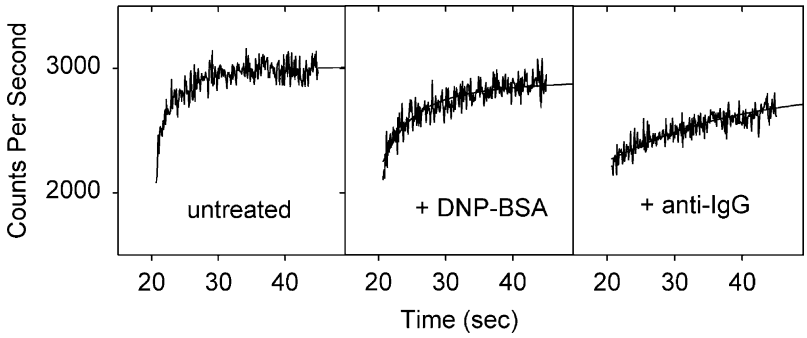

Fig. 3. Effects of FcεRI and MAFA crosslinking on MAFA lateral diffusion at 23 °C as probed by Er-G63 Fab. Fluorescence recovery traces shown represent averages of 10 individual cell measurements obtained in a single experiment. The *y*-axes of the middle and right panels have been adjusted vertically to align recovery traces. Crosslinking FcεRI by DNP_{11}-BSA reduced MAFA's diffusion coefficient from $(1.90 \pm 0.24) \times 10^{-10}$ on untreated cells to $(0.76 \pm 0.23) \times 10^{-10}\,cm^2\,s^{-1}$ after DNP_{11}-BSA treatment. As would be expected, crosslinking MAFA through G63Fab and anti-IgG produced a much larger effect on the MAFA diffusion coefficient, reducing it almost 10-fold to $0.19 \pm 0.03\,cm^2\,s^{-1}$.

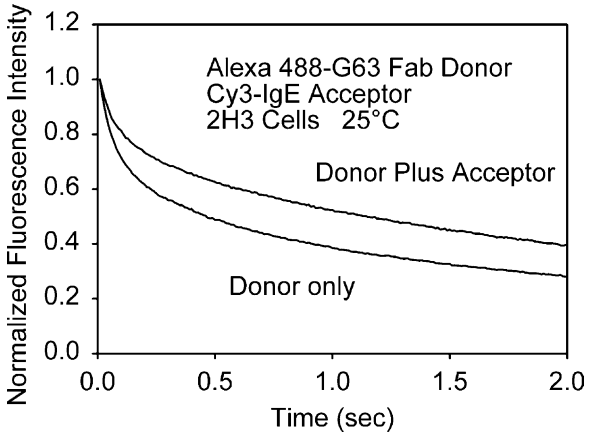

Fig. 4. Evaluation of FRET from Alexa 488-G63 Fab to Cy3-IgE on 2H3 cells by donor photobleaching. Energy transfer between donor and acceptor chromophores slows the rate of irreversible donor photobleaching relative to that on cells bearing only donor (Young et al., 1994). Thus, comparison of normalized decay kinetics for the two cell groups in the particular experiment shown indicates 37% energy transfer. Substantial variability in energy transfer is observed between experiments and this may reflect variation with cell culture density, time in culture, etc. of surface expression of FcεRI and MAFA leading to different degrees of equilibrium association and, thus, of FRET.

also shown to cause inhibition, we wondered nonetheless whether the Fcγ domain of this IgG_1-class antibody might also be involved in cell surface interaction, since 2H3 cells also express Fcγ receptors. Table 1 shows that intact mAb G63 exhibits higher anisotropies and a slower rotational correlation time than its $F(ab')_2$ derivative. These differences suggest interaction of intact G63's Fcγ domain with a membrane entity such as FcγRII (CD32) (Bocek et al., 1995).

The mAb G63 is of the IgG_1 subtype (Soto and Pecht, 1988) which has the highest affinity for the Type IIB Fcγ receptor (FcγRIIB). This receptor is known to inhibit activation signals produced by ITAM-containing receptors upon co-clustering with ITIM-containing receptors (Daeron, 1997). Thus, it is attractive to suppose that inhibition of the secretory response by mAb G63 might be potentiated by the interaction of its Fcγ domain with other ITIM-containing receptors also expressed on 2H3 cells.

3.5. Some fraction of MAFA appears constitutively associated with lipid rafts

In preliminary experiments we have investigated the possible raft localization of MAFA on cells subjected to clustering of FcεRI and/or MAFA. Since resting FcεRI are isolated in high density fractions but move into rafts upon aggregation, receptor-associated MAFA should exhibit similar behavior. Density gradient centrifugation of cell detergent extracts was conducted as described in Material and Methods. In parallel studies we performed TPA measurements of protein rotation before and after ganglioside G_{M1} crosslinking by biotinylated cholera toxin B subunit and streptavidin. Results of these experiments are shown in Table 2. Peak concentrations of both FcεRI and MAFA appear at approximately 40% sucrose when isolated from untreated cells but are isolated in lower-density fractions (approximately 30%) after the receptor is crosslinked with DNP-BSA. After pre-treatment with G63 mAb, MAFA also appears in lower density fractions, peaking at approximately 33%. These results suggest that clustering either species moves MAFA in raft domains.

Table 1
Comparison of rotational parameters for MAFA-bound G63 Fab and $F(ab')_2$ at 4 °C

	Initial anisotropy r_0	Limiting anisotropy r_∞	Rotational correlation time (μs)	n
Er-G63 mAb	0.065 ± 0.007	0.054 ± 0.005	80 ± 14	3
Er-G63 $F(ab')_2$	0.061 ± 0.009	0.044 ± 0.006	49 ± 6	3

Table 2
Association of MAFA with lipid rafts

Aggregation of FcεRi[a]	Aggregation of MAFA[b]	Sucrose % for FcεRi[c]	Sucrose % for MAFA[c]	Effect on IgE rotation[d]	Effect on MAFA rotation[d]
−	−	40	40	46 → 47	45 → 50
+	−	30	30	31 → 60	44 → 50
−	+	−	33	55 → 53	51 → 57

[a] FcεRI were aggregated by treatment with DNP_{11}-BSA, 200 ng/ml, 30 min, 37 °C, in density gradient centrifugation experiments or 1 μg/ml, 1 h, 4 °C, in protein rotation experiments.

[b] MAFA was aggregated by treatment with G63mAb, 100 nM, 30 min, 37 °C in density gradient centrifugation experiments or 30 nM G63 $F(ab')_2$, 1 h, 4 °C, then goat anti-mouse Fab, 14 μg/ml, 30 min, 37 °C, then rabbit anti-goat IgG μg/ml 30 min, 37 °C, in protein rotation experiments.

[c] Sucrose concentrations were determined from index of refraction measurements on gradient fractions. The values given represent locations of peak intensities on immunoblots for FcεRI by J17 mAb and for MAFA by G63 mAb, respectively.

[d] 1000 × limiting anisotropies for the indicated species before and after ("→") treatment with biotin-cholera toxin subunit B, 5 μg/ml, 1 h, 4 °C, then streptavidin, 4 μg/ml, 5 min, 37 °C.

Table 2 also shows that crosslinking ganglioside GM1, a raft-associated lipid, with biotinylated-cholera toxin B subunit (CTB) followed by streptavidin increases the limiting anisotropy of MAFA on unperturbed, FcεRI-clustered or MAFA-clustered cells. Interpretation of these results depends on how GM1 crosslinking affects FcεRI localization. Draber has observed (P. Draber, unpublished results) that CTB treatment causes FcεRI translocation into membrane raft fractions. In such a case, the sensitivity of MAFA rotation to CTB treatment further suggests pre-association of MAFA with FcεRI.

4. Discussion

In summary, we have shown that (1) MAFA rotational diffusion resembles that of FcεRI, though size suggests that MAFA should rotate much faster; (2) MAFA rotational and lateral diffusion are both restricted by allergen clustering of FcεRI, though not as much as by directly crosslinking MAFA by Ab; and (3) Fab-labeled MAFA exhibits spontaneous FRET to IgE. Thus, a substantial fraction of, but not all of, resting MAFA appears constitutively associated with FcεRI. Additionally, we see that the Fc domain of mAb G63 restricts rotation of MAFA-bound antibody, perhaps through interactions with receptors like FcγIIB. Finally, preliminary results suggest MAFA moves with FcεRI into rafts upon either FcεRI or MAFA aggregation.

Taken together, the above results support a model for MAFA's inhibitory action: MAFA clustering causes a transient increase in phosphorylation of its own ITIM tyrosyl residue. The tyrosyl-phosphorylated ITIM recruits phosphatases, primarily the SH2 domain-containing phosphatase SHIP (Xu et al., 2001), which deplete the membranal levels of signaling phosphatidyinositol phosphates produced upon FcεRI clustering. MAFA's possible co-localization with clustered FcεRI in lipid rafts could facilitate this depletion. We might speculate that: (1) there is at least one MAFA molecule per lipid raft; (2) SHIP's phosphatase activity is sufficiently high; and (3) the molecular targets of PIP_3 are largely raft-associated. In such a case, then each MAFA could significantly deplete PIP_3 levels in and around its raft. Thus a few MAFA molecules, efficiently targeted to, and subsequently phosphorylated in, lipid rafts could inhibit signaling by a much larger number of FcεRI.

Acknowledgements

The Authors are grateful to Mr. Arieh Licht for preparation of mAb G63 and other reagents used in these studies. This work was supported in part by a United States-Israel Binational Science Foundation grant 96-00445 to I.P. and B.G.B., by NIH grant HD23236 to D.A.R. and by NSF grant MCB-9807822 to B.G.B.

References

Baniyash, M., Eshhar, Z., 1984. Inhibition of IgE binding to mast cells and basophils by monoclonal antibodies to murine IgE. Eur. J. Immunol. 14, 799–807.

Barisas, B.G., Wade, W.W., Jovin, T.M., Arndt-Jovin, D., Roess, D.A., 1999. Dynamics of molecules involved in antigen presentation: Effects of Fixation. Mol. Immunol. 36, 701–708.

Bocek Jr., P., Draberova, L., Draber, P., Pecht, I., 1995. Characterization of Fc gamma receptors on rat mucosal mast cells using a mutant Fc epsilon RI-deficient rat basophilic leukemia line. Eur. J. Immunol. 25, 2948–2955.

Carsten, M.E., Eisen, H.N., 1953. The interaction of dinitrobenzene derivatives with bovine serum albumin. J. Amer. Chem. Soc. 75, 4451–4456.

Daeron, M., 1997. Fc receptor biology. Annu. Rev. Immunol. 15, 203–234.

Field, K.A., Holowka, D., Baird, B., 1995. Fc-epsilon-RI-mediated recruitment of p53/56lyn to detergent-resistant membrane domains accompanies cellular signaling. Proc. Natl. Acad. Sci. U.S.A. 92, 9201–9205.

Guthmann, M.D., Tal, M., Pecht, I., 1995a. A secretion inhibitory signal transduction molecule on mast cells is another C-type lectin. Proc. Natl. Acad. Sci. U.S.A. 92, 9397–9401.

Guthmann, M.D., Tal, M., Petch, I., 1995b. A new member if the C-type lectin familly is a modulator of the mast cell secretory response . Int. Arch. Allergy Immunol. 107, 82–86.

Johnson, G.D., Holborow, E.J., 1986. Preparation and use of flourochrome conjugates. In: Weir, D.M. (Ed.), Handbook of Experimental Immunology, Blackwell, Boston, pp. 28.1–28.21.

Johnson, P., Garland, P.B., 1981. Depolarization of fluorescence depletion. A microscopic method for measuring rotational diffusion of membrane proteins on the surface of a single cell. Feder. Eur. Biochem. Soc. Lett. 132, 252–256.

Jurgens, L., Arndt-Jovin, D., Pecht, I., Jovin, T.M., 1996. Proximity relationships between the type I receptor for Fc (FcRI) and the mast cell function-associated antigen (MAFA) studied by donor photobleaching fluorescence resonance energy transfer microscopy. Eur. J. Immunol. 26, 84–91.

Kubitscheck, U., Kircheis, M., Schweitzer-Stenner, R., Dreybrodt, W., Jovin, T.M., Pecht, I., 1991. Fluorescence resonance energy transfer on single living cells: application to binding of monovalent haptens to cell-bound immunoglobulin E. Biophys. J. 60, 307–318.

Munnelly, H.M., Brady, C.J., Hagen, G.M., Wade, W.F., Roess, D.A., Barisas, B.G., 2000. Rotational and lateral dynamics of I-A(k) molecules expressing cytoplasmic truncations. Int. Immunol. 12, 1319–1328.

Munnelly, H.M., Roess, D.A., Wade, W.F., Barisas, B.G., 1998. Interferometric fringe fluorescence photobleaching recovery interrogates entire cell surfaces. Biophys. J. 75, 1131–1138.

Ortega, E., Pecht, I., 1988. A monoclonal antibody that inhibits secretion from rat basophilic leukemia cells and binds to a novel membrane component. J. Immunol. 141, 4324–4332.

Philpott, C.J., Rahman, N.A., Kenny, N., Barisas, B.G., Roess, D.A., 1995. Rotational dynamics of luteinizing hormone receptors on bovine and ovine luteal cell plasma membranes. Biol. Reprod. 53, 645–650.

Rong, X., Pecht, I., 1996. Clustering the mast cell function-associated antigen (MAFA) induces tyrosyl phosphorylation of the Fc epsilon RI-beta subunit. Immunol. Lett. 54, 105–108.

Schweitzer-Stenner, R., Engelke, M., Licht, A., Pecht, I., 1999. Mast cell stimulation by co-clustering the type I Fc receptors with mast cell function associated antigens. Immunol. Lett. 68, 71–78.

Song, J., Hagen, G.M., Roess, D.A., Pecht, I., Barisas, B.G., 2002. Time-resolved phosphorescence anisotropy studies of the mast cell function-associated antigen and its interactions with the type I Fcε receptor. Biochemistry 41, 881–889.

Soto, E.O., Pecht, I., 1988. A monoclonal antibody that inhibits secretion from rat basophilic leukemia cells and binds to a novel membrane component. J. Immunol. 141, 4324–4332.

Xu, R., Abramson, J., Fridkin, M., Pecht, I., 2001. SH2 domain-containing inositol polyphosphate 5′-phosphatase is the main mediator of the inhibitory action of the mast cell function-associated antigen. J. Immunol. 167, 6394–6402.

Xu, R., Pecht, I., 2001. The protein tyrosine kinase syk activity is reduced by clustering the mast cell function-associated antigen. Eur. J. Immunol. 31, 1571–1581.

Young, R.M., Arnette, J.K., Roess, D.A., Barisas, B.G., 1994. Quantitation of fluorescence energy transfer between cell surface proteins via fluorescence donor photobleaching kinetics. Biophys. J. 67, 881–888.